

Design of Geometric Molecular Bonds

David Doty and Andrew Winslow

Abstract—An example of a *nonspecific* molecular bond is the affinity of any positive charge for any negative charge (like-unlike), or of nonpolar material for itself when in aqueous solution (like-like). This contrasts *specific* bonds such as the affinity of the DNA base A for T, but not for C, G, or another A. Recent experimental breakthroughs in DNA nanotechnology [13], [22] demonstrate that a particular nonspecific like-like bond (“blunt-end DNA stacking” that occurs between the ends of any pair of DNA double-helices) can be used to create specific “macrobonnds” by careful geometric arrangement of many nonspecific blunt ends, motivating the need for sets of macrobonnds that are *orthogonal*: two macrobonnds not intended to bind should have relatively low binding strength, even when misaligned.

To address this need, we introduce *geometric orthogonal codes* that abstractly model the engineered DNA macrobonnds as two-dimensional binary codewords. While motivated by completely different applications, geometric orthogonal codes share similar features to the *optical orthogonal codes* studied by Chung, Salehi, and Wei [7]. The main technical difference is the importance of 2D geometry in defining codeword orthogonality.

I. INTRODUCTION

A. Experimental DNA nanotechnology

DNA nanotechnology began in the 1980s when Seeman [19] showed that artificially synthesized DNA strands could be designed to automatically self-assemble nanoscale structures, rationally designed through the choice of DNA sequences. In the past 20 years, the field has witnessed a dramatic surge in the development of basic science, *in vitro* applications, such as chemical oscillators and molecular walkers, and *in vivo* applications, such as drug delivery, cellular RNA sensing, and genetically encoded structures [6].

A technological pillar of the field is *DNA origami*, developed by Rothemund [17], a simple, fast, inexpensive, and reliable method for creating artificial 2D and 3D DNA structures, with a control resolution of a few nanometers. DNA origami requires a single long *scaffold* strand of DNA; the most commonly used is the 7249-nucleotide single-stranded genome of the bacteriophage virus M13mp18, widely and cheaply available from many biotech companies. The scaffold is mixed with a few hundred shorter (≈ 32 nt) synthesized strands called *staples*, each of which is designed to bind (through Watson-Crick complementarity) to 2-3 regions of the scaffold. Via thermal annealing, the staples fold the scaffold strand into a shape dictated by the choice of staple sequences, hence the term *origami*. The process is illustrated in Figure 1(a), with the results shown in Figure 1(b).

A preliminary draft of this article appeared as [10].

D. Doty was supported by NSF grants 1317694, 1219274, 1442454, and the Molecular Programming Project under NSF grant 1619343.

D. Doty is with the Computer Science department of the University of California, Davis, doty@ucdavis.edu.

A. Winslow is with the Departement d’Informatique of Université Libre de Bruxelles, awinslow@ulb.ac.be.

Although the Watson-Crick pairing of bases between two single strands of DNA is very specific, DNA is known to undergo other, less specific interactions. One well-studied interaction is called a *stacking bond*, formed when *any* pair of terminated double helices — known as *blunt ends* — face each other, as shown in Figure 1(c). Since two edges of a standard DNA origami rectangle consist entirely of blunt ends, DNA origami rectangles are known to bind along their edges to form long polymers of many origamis, despite the fact that no hybridization between single strands occurs between them. One way to avoid stacking between origamis is to leave out staple strands along the edge, so that rather than blunt ends, there are single-stranded loops of the scaffold strand [17].

Woo and Rothemund [22] turned unintended origami stacking into a feature with the following idea: leave out *some* of the staples along the edge, but keep others; see Figure 1(d). Although individual blunt ends bind nonspecifically to others, the only way for *all* blunt ends along an edge to bind is with matching blunt ends on another origami in the same relative positions. Thus, geometric placement of blunt ends makes the entire side of an origami into a specific “macrobond”. Figure 1(d) shows how this approach enforces that a set of origamis bind to form only intended arrangements.

The idea extends from 2D origami rectangles with 1D edges, to 3D origami boxes with 2D rectangular faces as demonstrated by Gerling, Wagenbauer, Neuner, and Dietz [13].¹ They rationally design polymers of many origamis with prescribed sizes and shapes such as the 4-mer ABCD shown in Fig. 1(e).

The preceding description of macrobonnds is idealized: other mechanisms may permit unintended pairs of macrobonnds to bind spuriously. Figure 1(f) shows two macrobonnds aligning sufficiently many blunt ends to attach stably via two such mechanisms: *flexibility* of DNA helices and *misalignment* of macrobonnds. This paper is an attempt to attack the latter problem with coding theory.

B. Statement of model and main result

Although inspired by work in DNA nanotechnology, the design of specific macrobonnds formed by geometric arrangements of nonspecific bonds is fundamental and likely to be part of the future of nanotechnology, even if based on substrates other than DNA. We abstract away several details of DNA origami in mathematically formulating the problem.

Let $[n] = \{0, 1, \dots, n-1\}$. We model each 2D face of a monomer (e.g., a DNA origami) as a discrete $n \times n$ square $[n]^2$, with n representing the placement resolution of nonspecific

¹The motif is slightly different. Rather than helices orthogonal to the origami face, they are parallel. As seen in Figure 1(e), pairs of whole helices protrude and a complementary face has a two-helix “gap” into which these helices fit to form four total stacking bonds.

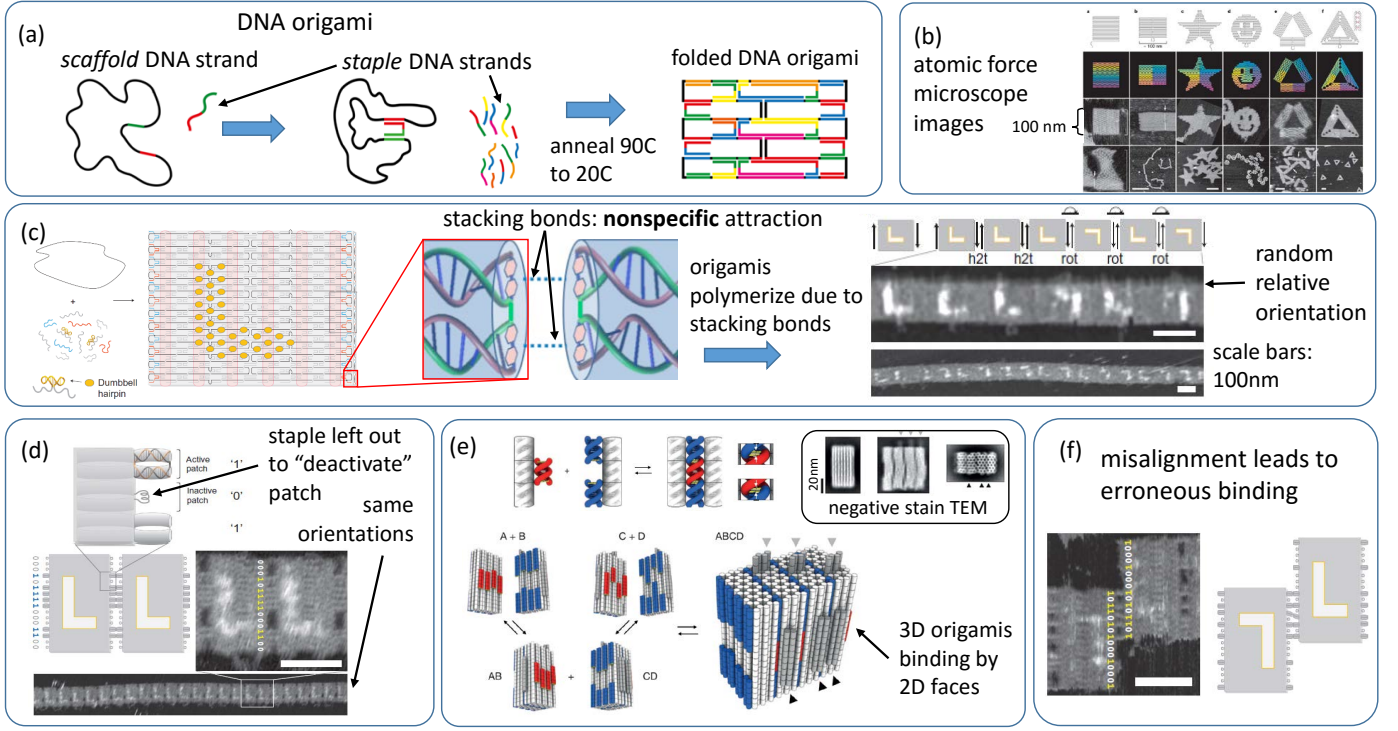


Fig. 1. Illustration of DNA origami and geometrically programmable stacking bonds. (a) DNA origami illustration (source: <http://openwetware.org/wiki/Biomod/2014/Design>). (b) Atomic force microscope images of nanoscale shapes assembled by DNA origami technique (source: [17]). (c) Stacking bonds are nonspecific attraction occurring between the *ends* of two DNA helices, such as those that appear on the edges of a DNA origami causing origamis to form long chains (*polymerize*) in solution. Markers on the origami surface (an asymmetrical *L* shape) reveal that the orientation of origamis in a polymer is random; i.e., some are “upside down” relative to others (source: <http://openwetware.org/wiki/Biomod/2014/Kansai/Experiment> and [22]). (d) By removing certain stacking bonds at specific locations to create a binary pattern on the edge of a DNA origami, the whole edge becomes a specific “macrobond” that binds most strongly to another edge with the same pattern; in this case, the left side of an origami binds favorably to the right side, and less favorably to another left side (source: [22]). (e) The technique also works to bind 3D origami using 2D patterns of stacking bonds on their faces, using a slightly different motif than in part (d). The placement of the nonspecific bonds gives the entire face a higher affinity for another face with a complementary pattern (source: [13]). (f) One source of error is the matching of many stacking bonds between two misaligned faces (source: [22]).

bonds, called *patches*. A *macrobond* is a subset $M \subseteq [n]^2$. Given a vector $\vec{v} \in \mathbb{Z}^2$, $M + \vec{v} = \{ \vec{m} + \vec{v} \mid \vec{m} \in M \}$ denotes M translated by \vec{v} . A parameter $w \in \{2, \dots, n^2\}$ denotes the *target strength* (or *weight*). A parameter $\lambda \in \{1, \dots, w - 1\}$ denotes the *orthogonality strength threshold*. An (n, w, λ) *geometric orthogonal code* is a set of macrobonds $\mathcal{M} = \{M_1, \dots, M_\ell\}$, where each $M_i \subseteq [n]^2$ and $|M_i| = w$, so that for all $1 \leq i < j \leq \ell$, two conditions hold:

low cross-correlation: $\forall \vec{v} \in \mathbb{Z}^2, |M_i \cap (M_j + \vec{v})| \leq \lambda$.

low auto-correlation: $\forall \vec{v} \in \mathbb{Z}^2 \setminus \{\vec{0}\}, |M_i \cap (M_i + \vec{v})| \leq \lambda$.

Informally, an (n, w, λ) geometric orthogonal code is a set of macrobonds with n^2 available space for potential binding sites, total binding strength w , and spurious binding strength limited to at most λ . As with any code, the goal is to maximize the number of codewords $|\mathcal{M}|$. The main result of this paper is that for all $n, \lambda \in \mathbb{Z}^+$ with n a prime and $2 \leq \lambda < n$, there exists an efficiently computable (n, n, λ) geometric orthogonal code \mathcal{M} with $|\mathcal{M}| = n^{\lambda-1} - n^{\lambda-2}$.

Examine the physical implementation of patches shown in Figure 1(e), and observe that a “bump” patch on one macrobond cannot insert into a “hole” patch on another macrobond if they are rotated relative to each other, *un-*

less the rotation is by 180° , i.e., flipped along each axis.² (Otherwise the blunt ends will not be flush.) To model this, we define an (n, w, λ) *geometric flipping orthogonal code* to be an (n, w, λ) geometric orthogonal code that, defining $\text{flip}(M_i) = \{ (n-1-x, n-1-y) \mid (x, y) \in M_i \}$, also obeys $|\text{flip}(M_i) \cap (M_j + \vec{v})| \leq \lambda$ for all $1 \leq i \leq j \leq \ell$ and all $\vec{v} \in \mathbb{Z}^2$. We demonstrate codes that obey this extra constraint as well.

C. Related work

The most directly related theoretical work are the binary *optical orthogonal codes* studied by Chung, Salehi, and Wei [7], which minimize the number of overlapping 1’s (analogous to our nonspecific patches) between codewords; overlapping 0’s (analogous to neutral non-binding sites) are not penalized. Also, these codes consider all possible translations of

²There are physical reasons to dismiss this possibility, since the energy of a stacking bond appears to weaken if the relative rotation angle of the two DNA phosphate backbones are rotated 180° relative to each other: see the image on the right of Figure 1(c), where only two of four possible orientations appear. The other two would put the *L* pattern *underneath* the origami; presumably they are absent due to weaker stacking energy of rotated helices. Nonetheless, if one imagines a mixture of different angles being used in different patches, rather than only one angle as in [22], then it may be reasonable to assume a worst-case scenario in which a 180° rotation could make any of the patch backbone angles match between two macrobonds.

codewords; a codeword requires orthogonality not only to translations of other codewords (cross-correlation) but also to nonzero translations of itself (auto-correlation).

The major difference between optical orthogonal codes and our work is the geometric nature of our codes.³ Each codeword represents a 2D face of a 3D molecular structure, so translations in both x and y coordinates must be considered.

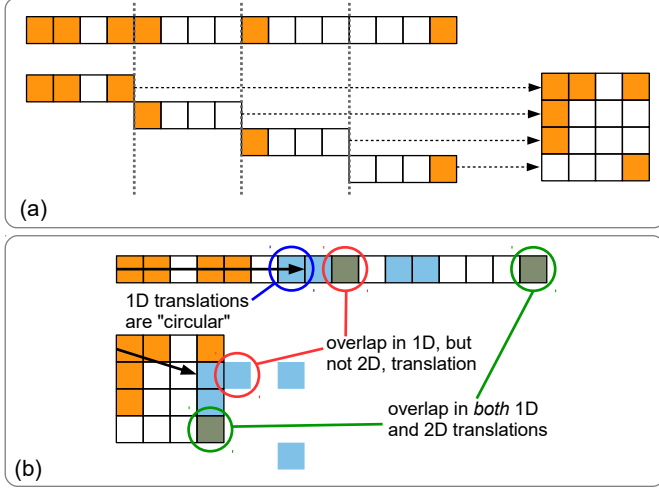


Fig. 2. (a) Each 1D codeword of an optical orthogonal codeword of length n^2 can be interpreted as a 2D macrobond (a codeword of a geometric orthogonal code) in a natural way by interpreting blocks of length n as rows of the macrobond. (b) Each translation of a 1D codeword by $k \in \mathbb{Z}^+$ can be interpreted as a translation of the equivalent 2D macrobond by $(x, y) = (k \bmod n, \lfloor k/n \rfloor)$. An example 1D translation by $+7$ is shown in blue, which corresponds to translating the 2D macrobond by $(+3, -1)$. Each overlap between the original (orange) and the translated (blue) 2D macrobonds corresponds to an overlap between the original and translated 1D codewords. (See overlaps circled in green.) However, the converse does not hold: an overlap in the 1D codewords is not necessarily an overlap between the 2D codewords. (See red circles.) Also, in an optical orthogonal code, translations are “circular”: each patch that moves off the end of the codeword wraps back to the beginning, resulting in further potential overlaps in the 1D case that are not counted in the 2D case. (See blue circle.) Thus, each (n^2, w, λ) optical orthogonal code, interpreting each codeword as a 2D macrobond as in (a), is a (n, w, λ) geometric orthogonal code, but the converse does not hold.

Despite these differences, one could imagine applying the optical orthogonal codes of [7] directly to our problem setting. Indeed, every (n^2, w, λ) optical orthogonal code is in fact an (n, w, λ) geometric orthogonal code by interpreting each 1D codeword as the concatenation of the n rows of a 2D codeword. Figure 2 shows how this interpretation works, and why the two types of codes are not equivalent. Specifically, the constraints of 1D optical orthogonal codes are stronger than what is needed for 2D geometric orthogonal codes.

Table I compares the (n, n, λ) geometric orthogonal code sizes of our main construction to the (n^2, n, λ) optical orthogonal code sizes of the best construction (Theorem 2) of [7],

³Another difference with our setting is that optical orthogonal codes are more stringent in defining orthogonality under translation. In [7], translations are assumed to be modulo the codeword size, whereas in our setting such “wrapping” does not make sense: a molecular structure α moving off the end of another structure β does not appear on the opposite side of β , hence could not contribute to the binding strength. They also use different parameters to bound auto-correlation and cross-correlation, but for the setting we are modeling, these both correspond to spurious molecular bonds, so it makes sense to use the same threshold for each.

showing that we achieve larger code sizes in most tested cases. There has been subsequent work on optical orthogonal codes. However, much of it is for the special case of $\lambda = 1$ and/or $w = 4$ [3], [11], [12], [23], [9, Section V.9] or other special cases for single values of parameters [1], [2], [4], [8], [21].

Two-dimensional optical orthogonal codes have been studied [5], [16], [20]. The 2D nature of these codes reflects the fact that two different variables (e.g., time and wavelength) determine where 1’s and 0’s appear in the codeword. However, these techniques do not apply directly to our problem, since they consider only translation in one dimension (time) while we must consider simultaneous translations along both dimensions. In other words, the distinction of having two *identical*, *spatial* dimensions is important.

Huntley, Murugan, and Brenner [15] have also studied specific engineered molecular bonds from an information theory perspective. They study a different model in which translation is disallowed. They study “color” coding: extending the patches to allow some specificity, so that only equal-color patches can bind; see Section III for a discussion of this issue. They compare color coding with “shape” coding: allowing the shape of a 1D edge to be nonflat, thus providing steric hindrance as an additional mechanism to prevent unintended binds (also discussed as an open question in Section III). They run simulations to show that randomly selected shape codes have greater size than randomly selected color codes.

II. RESULTS

A. Lower bounds

The following theorem shows how to construct geometric orthogonal codes *without* the flipping constraint.

Theorem II.1. *For each prime $n \in \mathbb{N}$ and $\lambda \in \{2, \dots, n-1\}$, there is an (n, n, λ) geometric orthogonal code of size $n^{\lambda-1} - n^{\lambda-2}$.*

Proof. Translation by a vector $\vec{v} = (\delta_x, \delta_y) \in \mathbb{Z}^2$ with $|\delta_x|$ or $|\delta_y| \geq n$ implies correlation is 0. So assume $|\delta_x|, |\delta_y| < n$.

Let \mathbb{F}_n denote the finite field of order n , where n is prime, which can be interpreted as normal integer addition and multiplication modulo n , with field elements $\mathbb{F}_n = [n]$. Each macrobond is defined by a degree- λ polynomial $p(x) = a_\lambda x^\lambda + a_{\lambda-1} x^{\lambda-1} + \dots + a_1 x + a_0$ over \mathbb{F}_n , where each coefficient obeys $a_i \in \mathbb{F}_n$, $a_{\lambda-1} = a_0 = 0$, and $a_\lambda \neq 0$.

For a given polynomial p , the corresponding macrobond $M_p = \{ (x, p(x)) \mid x \in \mathbb{F}_n \}$, i.e., a patch in column x on row $p(x)$. There are $(n-1)n^{\lambda-2} = n^{\lambda-1} - n^{\lambda-2}$ such polynomials, since there are $n-1$ choices for a_λ and $n^{\lambda-2}$ choices for $a_{\lambda-2}, a_{\lambda-3}, \dots, a_1$.

It remains to prove that this code has auto-correlation and cross-correlation at most λ . The same argument will work for both. For mathematical convenience we equivalently consider translating by $(-\delta_x, \delta_y)$. Suppose there exist macrobonds M_p and M_q with $p(x) = \sum_{i=0}^{\lambda} a_i x^i$ and $q(x) = \sum_{i=0}^{\lambda} b_i x^i$ that intersect on more than λ patches under translation $(-\delta_x, \delta_y)$. We will prove that $a_i = b_i$ for all $i \in \{0, \dots, \lambda\}$ and that $\delta_x = \delta_y = 0$, simultaneously establishing that the code has auto-correlation and cross-correlation at most λ .

Translating the polynomial p by $(-\delta_x, \delta_y)$ results in the polynomial $p(x+\delta_x)+\delta_y$. If this intersects with the polynomial $q(x)$ on more than λ points, then by the fundamental theorem of algebra, $p(x+\delta_x)+\delta_y$ is identically $q(x)$, i.e., they have the same coefficients.

The constant term of $p(x+\delta_x)+\delta_y$ is $a_0+\delta_y$, and the constant term of $q(x)$ is b_0 . Since the coefficients of p and q are equal, $a_0+\delta_y=b_0$, but since $a_0=b_0=0$, this implies $\delta_y=0$ also. Thus $p(x+\delta_x)+\delta_y=p(x+\delta_x)$.

Note that

$$\begin{aligned} p(x+\delta_x) &= \sum_{i=0}^{\lambda} a_i (x+\delta_x)^i \\ &= \sum_{i=0}^{\lambda} a_i \sum_{k=0}^i \binom{i}{k} \delta_x^{i-k} x^k \quad (\text{binomial theorem}) \\ &= \sum_{k=0}^{\lambda} x^k \sum_{i=k}^{\lambda} a_i \binom{i}{k} \delta_x^{i-k} \end{aligned}$$

Thus, if $p(x+\delta_x)$ and $q(x)$ have the same coefficients, then the $q(x)$ coefficient of the term x^k is $b_k = \sum_{i=k}^{\lambda} a_i \binom{i}{k} \delta_x^{i-k}$.

In particular $b_{\lambda-1} = \sum_{i=\lambda-1}^{\lambda} a_i \binom{i}{\lambda-1} \delta_x^{i-(\lambda-1)} = a_{\lambda-1} \binom{\lambda-1}{\lambda-1} \delta_x^{\lambda-1-(\lambda-1)} + a_{\lambda} \binom{\lambda}{\lambda-1} \delta_x^{\lambda-(\lambda-1)} = a_{\lambda-1} + a_{\lambda} \lambda \delta_x$. Since $a_{\lambda-1} = b_{\lambda-1} = 0$, this implies $a_{\lambda} \lambda \delta_x = 0$. Since $\lambda, a_{\lambda} \neq 0$, this implies $\delta_x = 0$.

In other words, the total translation must be zero. Thus every macrobond has low auto-correlation. Since $\delta_x = \delta_y = 0$, it must be that $p = q$ and thus $M_p = M_q$, so any pair of *unequal* macrobonds have low cross-correlation. \square

We now show how to obtain a geometric *flipping* orthogonal code, using similar techniques to the proof of Theorem II.1.

Theorem II.2. *For each prime $n \in \mathbb{N}$ and $\lambda \in \{2, \dots, n-1\}$, there is an (n, n, λ) geometric flipping orthogonal code of size $(n^{\lambda-1} - n^{\lambda-2} - n^{\lceil \lambda/2 \rceil})/2$ if n is odd, and $(n^{\lambda-1} - n^{\lambda-2} - 2^{\lceil \lambda/2 \rceil + 1} n^{\lceil \lambda/2 \rceil})/2$ if n is even.*

Proof. The construction is a modification of Theorem II.1 obtained by taking a subset of the code that avoids high correlation in the new orientation. Assume that there exist polynomials p and q and a translation vector (δ_x, δ_y) such that M_q has correlation $> \lambda$ with $\text{flip}(M_p) + (\delta_x, \delta_y)$. By definition, $\text{flip}(M_p) = \{ (n-1-x, n-1-p(x)) \mid x \in \mathbb{F}_n \} = \{ (x, n-1-p(n-1-x)) \mid x \in \mathbb{F}_n \}$, so by the fundamental theorem of algebra, $n-1-p(n-1-x+\delta_x)+\delta_y = q(x)$ for all $x \in \mathbb{F}_n$.

The $x^{\lambda-1}$ term of $q(x)$ is 0 by construction. Expanding the two leading terms of $n-1-p(n-1-x+\delta_x)+\delta_y$ with this constraint implies that $a_{\lambda} \lambda (n-1+\delta_x)(-1)^{\lambda} = 0$. Then since $\lambda, a_{\lambda}, (-1)^{\lambda} \neq 0$, it must be that $n-1+\delta_x = 0$. So $\delta_x = 1$ and $n-1-p(n-1-x+\delta_x)+\delta_y = n-1-p(-x)+\delta_y$.

Expanding all terms of $n-1-p(-x)+\delta_y$ and $q(x)$ leads to $n-1+\delta_y = n-1+a_0+\delta_y = b_0 = 0$. So $\delta_y = 1$ and thus $n-1-p(n-1-x+\delta_x)+\delta_y = n-p(n-x) = -p(-x) = q(x)$. Expanding these polynomials implies that for all i , $a_i(-1)^{i+1} = b_i$.

Define a *complement* of a polynomial $p(x)$ to be $\sum_{i=1}^{\lambda} a_i(-1)^{i+1}x^i$, i.e. the polynomial $q(x)$ such that

$-p(-x) = q(x)$. As the above shows, the current code allows two macrobonds to have correlation $> \lambda$ points if one of them is flipped, but only if the two corresponding polynomials are complements. Observe that every polynomial has a unique complement, and some polynomials are complements of themselves. Self-complement polynomials have auto-correlation more than λ and complementary pairs have cross-correlation more than λ . A flipping code can be obtained by taking any subset of the code that contains no polynomial and its complement.

A self-complementary polynomial is one in which for all even i , $a_i + a_i = 0$. If n is odd, this occurs only if $a_i = 0$, and if n is even, then it also occurs if $a_i = n/2$. Thus, the number of self-complementary polynomials is at most $n^{\lceil \lambda/2 \rceil}$ when n is odd and, since there are two choices for each even i coefficient, the number is $2^{\lceil \lambda/2 \rceil + 1} n^{\lceil \lambda/2 \rceil}$ when n is even.

So first remove all such self-complementary polynomials from the code. Of all the remaining, each has a unique complementary polynomial; remove one of them arbitrarily, cutting the number of remaining in half. So the flipping code has size $(n^{\lambda-1} - 1 - n^{\lceil \lambda/2 \rceil})/2$ for odd n , and $(n^{\lambda-1} - 1 - 2^{\lceil \lambda/2 \rceil + 1} n^{\lceil \lambda/2 \rceil})/2$ for even n . \square

Note that the proofs of Theorems II.1 and II.2 use finite field arithmetic only for fields of prime size, even though there are finite fields of size p^m for any prime p and $m \in \mathbb{Z}^+$. This is due to our technique of mapping the field elements to the integers $\{0, 1, \dots, n-1\}$ in such a way that translations in the x and y direction can be interpreted as changes in the underlying field elements. To make the correspondence straightforward, the characteristic of the field (the number of times the multiplicative identity 1 can be added before a repetition) must be equal to the field size, which is true exactly when the field size is prime. For prime size fields, translating x by the integer m is the same as adding 1 to x , m times in a row. Otherwise, translation from a point (x, y) to a point (x', y') , where (for example), $x' - x$ is greater than the field's characteristic but less than its size, would not be interpretable as mapping the element x to x' by repeated addition, and would invalidate the parts of the proof that reason about the effects of translation on the underlying polynomial evaluation.

B. Upper bounds

The following theorem shows an upper bound on the size of any geometric orthogonal code.

Theorem II.3. *Any (n, w, λ) geometric orthogonal code has size at most $\frac{1}{\binom{w}{\lambda+1}} \cdot \left[\binom{n^2-1}{\lambda} + \sum_{x_0=1}^{n-1} \sum_{y_0=1}^{n-1} \binom{n^2-x_0-y_0-1}{\lambda-1} \right]$.*

Proof. The approach is as follows. Imagine a “canonical” translation of $S \subseteq [n]^2$ so that it is “flush” against the x - and y -axes: S has at least one x -coordinate and one y -coordinate equal to 0. Two sets $S_1, S_2 \subseteq [n]^2$ are equal under some translation if and only if their canonical translations are equal.

Let \mathcal{M} be a (n, w, λ) geometric orthogonal code. Each macrobond has precisely $\binom{w}{\lambda+1}$ subsets of size $\lambda+1$, so there are $|\mathcal{M}| \cdot \binom{w}{\lambda+1}$ total induced subsets of size exactly $\lambda+1$. The code has auto- or cross-correlation more than

λ if and only if any two distinct of these subsets have equal canonical translations. We count the number of distinct canonically translated subsets of $[n]^2$ of size $\lambda + 1$, observing that $|\mathcal{M}| \cdot \binom{w}{\lambda+1}$ must be below this count to avoid repeating a subset by the pigeonhole principle.

For any $S \subseteq [n]^2$, define $S^\perp = S - (x_{\min}, y_{\min})$, where $x_{\min} = \min_{(x,y) \in S} (x)$ and $y_{\min} = \min_{(x,y) \in S} (y)$, to be the *canonical translation* of S . Note that $S^\perp \in [n]^2$, and S^\perp has at least one point on the x -axis and at least one point on the y -axis.

Each macrobond $M \subseteq [n]^2$ with $w = |M|$ has exactly $\binom{w}{\lambda+1}$ subsets of size exactly $\lambda + 1$. Denote these subsets as $M_{\lambda,1}, M_{\lambda,2}, \dots, M_{\lambda, \binom{w}{\lambda+1}}$. Note that macrobond M has autocorrelation $\leq \lambda$ if and only if $M_{\lambda,i}^\perp \neq M_{\lambda,j}^\perp$ for all $1 \leq i < j \leq \binom{w}{\lambda+1}$, and that macrobonds M and N have cross-correlation $\leq \lambda$ if and only if $M_{\lambda,i}^\perp \neq N_{\lambda,j}^\perp$ for all $1 \leq i, j \leq \binom{w}{\lambda+1}$. To avoid making any two of these translated subsets equal, an (n, w, λ) geometric orthogonal code \mathcal{M} obeys $|\mathcal{S}| = |\mathcal{M}| \cdot \binom{w}{\lambda+1}$, where $\mathcal{S} = \{M_{\lambda,i}^\perp \mid M \in \mathcal{M}, 1 \leq i \leq \binom{w}{\lambda+1}\}$. Thus $|\mathcal{M}| = \frac{1}{\binom{w}{\lambda+1}} |\mathcal{S}|$, and to prove the theorem, it suffices to show $|\mathcal{S}| \leq \binom{n^2-1}{\lambda} + \sum_{x_0=1}^{n-1} \sum_{y_0=1}^{n-1} \binom{n^2-x_0-y_0-1}{\lambda-1}$.

To bound $|\mathcal{S}|$, we simply count the number of canonical translations S^\perp of subsets $S \subseteq [n]^2$ with $|S| = \lambda + 1$. To be a canonical translation, S^\perp must have at least one point on the x -axis and at least one point on the y -axis. We count two disjoint subcases separately:

$(0,0) \in S^\perp$: There are $\binom{n^2-1}{\lambda}$ ways to pick the other λ points in S^\perp besides $(0,0)$.

$(0,0) \notin S^\perp$: Let $x_0 = \min_{(x,0) \in S^\perp} x$ and $y_0 = \min_{(0,y) \in S^\perp} y$. That is, x_0 and y_0 are, respectively, the smallest x - and y -coordinates of points in S^\perp whose other coordinate is 0. Because $(0,0) \notin S^\perp$, we have $x_0, y_0 > 0$. Once the two points defining x_0 and y_0 are fixed, there are $\lambda - 1$ other points to pick to be in S^\perp , and they must be picked from the set $A = \{(x,y) \in [n]^2 \mid (x=0 \implies y > y_0) \wedge (y=0 \implies x > x_0)\}$. Note that $|A| = (n-1)^2 + (n-x_0-1) + (n-y_0-1) = n^2 - x_0 - y_0 - 1$, where $(n-1)^2$ is the number of available points off both axes, and the terms $(n-x_0-1)$ and $(n-y_0-1)$ count the number of available points on each axis. There are thus $\binom{n^2-x_0-y_0-1}{\lambda-1}$ ways to pick these $(\lambda-1)$ points from A . Therefore there are $\sum_{x_0=1}^{n-1} \sum_{y_0=1}^{n-1} \binom{n^2-x_0-y_0-1}{\lambda-1}$ total sets in this subcase. \square

Table I compares the code size lower bound $L_{II.1}(n, \lambda) = n^{\lambda-1} - n^{\lambda-2}$ achieved by the algorithm of Theorem II.1 with the upper bound of Theorem II.3 (for the special case of $w = n$) $U_{II.3}(n, \lambda) = \frac{1}{\binom{n}{\lambda+1}} \left[\binom{n^2-1}{\lambda} + \sum_{x_0=1}^{n-1} \sum_{y_0=1}^{n-1} \binom{n^2-x_0-y_0-1}{\lambda-1} \right]$. Also shown is the lower bound $L_{\text{OOC}}(n^2, \lambda) = \frac{\binom{n^2}{n} - \frac{n-1}{2} \binom{n}{\lambda+1} \binom{n^2}{n-\lambda-1}}{n^2 \cdot \sum_{i=\lambda+1}^{\min(n^2-n, n)} \binom{n^2-n}{n-i} \binom{n}{i}}$ given by the (n^2, n, λ) optical orthogonal code construction of Theorem 2 of [7].

Theorem II.3 is our strongest upper bound but is unwieldy. The following corollary gives a weaker but simpler bound.

TABLE I
COMPARISON OF CODE SIZE LOWER BOUND $L_{II.1}(n, \lambda)$ OF THEOREM II.1 WITH CODE SIZE UPPER BOUND $U_{II.3}(n, \lambda)$ OF THEOREM II.3 AND LOWER BOUND $L_{\text{OOC}}(n^2, \lambda)$ GIVEN BY OPTICAL ORTHOGONAL CODE CONSTRUCTION OF THEOREM 2 OF [7].

n	λ	$L_{II.1}(n, \lambda)$	$U_{II.3}(n, \lambda)$	$L_{\text{OOC}}(n^2, \lambda)$
5	2	4	58	0
5	3	20	956	20
5	4	100	26,490	2,124
7	2	6	74	0
7	3	42	1,340	3
7	4	294	27,740	94
7	5	2,058	777,148	5,942
7	6	14,406	40,291,608	1,753,072
11	2	10	109	0
11	3	110	2,637	0
11	4	1,210	63,413	9
11	5	13,310	1,626,997	179
11	6	146,410	46,982,678	5,435
11	7	1,610,510	1,614,703,845	293,580
11	8	17,715,610	71,135,012,217	31,884,268
13	2	12	127	0
13	3	156	3,491	0
13	4	2,028	93,188	4
13	5	26,364	2,564,783	76
13	6	342,732	75,841,707	1,690
13	7	4,455,516	2,497,082,607	57,401
13	8	57,921,708	95,077,090,325	3,165,762
17	2	16	162	0
17	3	272	5,592	0
17	4	4,624	181,316	1
17	5	78,608	5,850,750	24
17	6	1,336,336	194,074,096	389
17	7	22,717,712	6,774,260,704	8,335
17	8	386,201,104	253,796,027,348	246,994
19	2	18	180	0
19	3	342	6,837	0
19	4	6,498	241,967	0
19	5	123,462	8,434,602	15
19	6	2,345,778	298,556,284	234
19	7	44,569,782	10,959,074,449	4,384
19	8	846,825,858	424,190,812,040	109,442
23	2	22	216	0
23	3	506	9,712	0
23	4	11,638	402,351	0
23	5	267,674	16,187,443	7
23	6	6,156,502	650,713,401	106
23	7	141,599,546	26,625,782,391	1,678
23	8	3,256,789,558	1,124,203,264,887	33,429

Corollary II.4. Any (n, w, λ) geometric orthogonal code has size at most $\frac{(\lambda+1)^2 e^{\lambda+1}}{w^{\lambda+1}} n^{2\lambda}$.

Proof. We use the bounds $\binom{m-1}{k} < \binom{m}{k}$, $\binom{m-1}{k-1} = \frac{k}{m} \binom{m}{k}$, and $\frac{m^k}{k^k} < \binom{m}{k} < \frac{e^k \cdot m^k}{k^k}$, for all $m, k \in \mathbb{Z}^+$. Then

$$\begin{aligned}
& \binom{n^2-1}{\lambda} + \sum_{x_0=1}^{n-1} \sum_{y_0=1}^{n-1} \binom{n^2-x_0-y_0-1}{\lambda-1} \\
& < \binom{n^2}{\lambda} + \sum_{x_0=1}^n \sum_{y_0=1}^n \binom{n^2-1}{\lambda-1} = \binom{n^2}{\lambda} + n^2 \binom{n^2-1}{\lambda-1} \\
& = \binom{n^2}{\lambda} + n^2 \frac{\lambda}{n^2} \binom{n^2}{\lambda} = (\lambda+1) \binom{n^2}{\lambda} < (\lambda+1) \frac{e^\lambda n^{2\lambda}}{\lambda^\lambda}.
\end{aligned}$$

Also, $\binom{w}{\lambda+1} > \frac{w^{\lambda+1}}{(\lambda+1)^{\lambda+1}}$. Combining these bounds with Theorem II.3, we have that the size of any (n, w, λ) geometric

orthogonal code is at most

$$\begin{aligned}
& \frac{1}{\binom{w}{\lambda+1}} \cdot \left(\binom{n^2-1}{\lambda} + \sum_{x_0=1}^{n-1} \sum_{y_0=1}^{n-1} \binom{n^2-x_0-y_0-1}{\lambda-1} \right) \\
& < \frac{1}{\frac{w^{\lambda+1}}{(\lambda+1)^{\lambda+1}}} \cdot (\lambda+1) \frac{e^\lambda n^{2\lambda}}{\lambda^\lambda} \\
& = \frac{(\lambda+1)e^\lambda}{w^{\lambda+1}} \cdot \frac{(\lambda+1)^{\lambda+1}}{\lambda^\lambda} \cdot n^{2\lambda} \\
& = \frac{(\lambda+1)^2 e^\lambda}{w^{\lambda+1}} \cdot \left(\frac{\lambda+1}{\lambda} \right)^\lambda \cdot n^{2\lambda} \\
& < \frac{(\lambda+1)^2 e^\lambda}{w^{\lambda+1}} \cdot e \cdot n^{2\lambda} = \frac{(\lambda+1)^2 e^{\lambda+1}}{w^{\lambda+1}} \cdot n^{2\lambda}. \quad \square
\end{aligned}$$

The following corollary applies in the special case where $n = w$.

Corollary II.5. *Any (n, n, λ) geometric orthogonal code has size at most $(\lambda+1)^2 e^{\lambda+1} n^{\lambda-1}$.*

Note that the upper bound of Corollary II.5 asymptotically matches the lower bound of Theorem II.1 when λ is constant with respect to n .

C. Random codes

Although simple and efficiently computable, it is worth asking if the technique of Theorem II.1 is overkill, compared to the most obvious way of attempting to generate codes: picking codewords at random. The next theorem shows that this approach yields much smaller codes if required to have one patch per column.

Theorem II.6. *Let $\epsilon > 0$ and let \mathcal{M} be a set of at least $\frac{\lambda+1}{n} \left(1 + \sqrt{2n^{(\lambda+1)} \ln \frac{1}{\epsilon}}\right)$ macrobonds, where each is selected uniformly at random from among those macrobonds with exactly one patch per column. With probability at least $1 - \epsilon$, \mathcal{M} is not a (n, n, λ) geometric orthogonal code.*

Proof. Note that macrobonds can be generated according to the distribution described in the theorem statement by iterating over each column and selecting one row uniformly at random to contain the patch in that column. Each selection of patches in nonoverlapping blocks of $\lambda+1$ consecutive columns can be viewed as a letter in an alphabet of size $n^{\lambda+1}$. Because the blocks are nonoverlapping, each letter selection is independent. Then each macrobond is partially specified by $\lfloor n/(\lambda+1) \rfloor$ letters defining the patch placements in the first $(\lambda+1)\lfloor n/(\lambda+1) \rfloor$ columns. If any letter is repeated (either within a macrobond, or between two different macrobonds), then the code has auto- or cross-correlation $> \lambda$.

The probability that a sequence of k randomly selected letters from an alphabet of size $n^{\lambda+1}$ does not contain a repeated letter is

$$\begin{aligned}
\prod_{i=0}^{k-1} (1 - i/n^{\lambda+1}) & \leq \prod_{i=0}^{k-1} e^{-i/n^{\lambda+1}} = e^{-\sum_{i=0}^{k-1} i/n^{\lambda+1}} \\
& = e^{-k(k-1)/(2n^{\lambda+1})} < e^{-(k-1)^2/(2n^{\lambda+1})}.
\end{aligned}$$

Thus the probability that a letter *does* repeat is at least $1 - e^{-(k-1)^2/(2n^{\lambda+1})}$. By algebra, the inequality $1 - \epsilon \leq 1 - e^{-(k-1)^2/(2n^{\lambda+1})}$ holds provided $k \geq 1 + \sqrt{2n^{\lambda+1} \ln \frac{1}{\epsilon}}$.

Since each macrobond induces $\lfloor n/(\lambda+1) \rfloor$ letters, a set of $\frac{\lambda+1}{n} \left(1 + \sqrt{2n^{(\lambda+1)} \ln \frac{1}{\epsilon}}\right)$ macrobonds induces $\frac{\lambda+1}{n} \left(1 + \sqrt{2n^{(\lambda+1)} \ln \frac{1}{\epsilon}}\right) \cdot \lfloor \frac{n}{\lambda+1} \rfloor \geq 1 + \sqrt{2n^{(\lambda+1)} \ln \frac{1}{\epsilon}}$ letters and thus with probability $\geq 1 - \epsilon$ contains a repetition. \square

Table II shows the result of testing random codes for $n = w$ and several prime values of n , comparing them to the proved theoretical bounds of Theorems II.1 and II.6. In each row of Table II, 100 trials were run. In each trial, codewords were generated by selecting n patches uniformly at random (without replacement) from the $n \times n$ square. Codewords were generated successively and added to the code until the auto- or cross-correlation of the code exceeded λ , and the code size recorded for the trial. The average (“ave”, rounded to nearest integer), median (“med”), standard deviation (“stddev”), and maximum (“max”) code sizes among the 100 trials are shown. These are compared to the lower bound $L_{II.1}(n, \lambda) = n^{\lambda-1} - n^{\lambda-2}$ achieved by the algorithm of Theorem II.1, as well as the randomized upper bound $U_{II.6}(n, \lambda, \frac{1}{2}) = \frac{\lambda+1}{n} \left(1 + \sqrt{2n^{(\lambda+1)} \ln 2}\right)$ proven in Theorem II.6 for random codes restricted to one patch per column (setting $\epsilon = \frac{1}{2}$).

Table III shows test results for random codes restricted to exactly one patch per column. In this case, each random codeword is generated by selecting, in each of n columns, one row uniformly at random in which to place a patch.

The results of Tables II and III suggest that the expected code size is much smaller than that achievable by our algorithm. There appears to be large variance in the code sizes achieved by generating codes at random. However, even the maximum among 100 trials, in nearly all cases, fell far below the code sizes given by the algorithm of Theorem II.1.

III. OPEN QUESTIONS

A number of directions for future work suggest themselves.

- 1) We chose to define a macrobond as a subset of an $n \times n$ square for convenience, and because it worked well with our proof technique using polynomials over finite fields. An obvious generalization is to find geometric orthogonal codes that work over $n \times m$ rectangles for $n \neq m$. Of course, one can simply remove rows/columns from, or add empty rows/columns to, a square macrobond while maintaining its auto- and cross-correlation, but it would be interesting to find a technique for generating codewords that is “naturally” defined over a rectangle or other geometry.
- 2) Our lower bound technique works for $w = n$, where w is the desired number of patches per macrobond. Generalize to arbitrary w .
- 3) Reduce the upper bound of Theorem II.3
- 4) Increase the lower bound of Theorems II.1 or II.2.
- 5) Generalize from primes to arbitrary $n \in \mathbb{Z}^+$.

TABLE II
EMPIRICAL TEST OF RANDOM CODES FOR $w = n$.

n	λ	ave	med	stddev	max	$L_{II.1}(n, \lambda)$	$U_{II.6}(n, \lambda, \frac{1}{2})$
5	2	2	2	1.2	6	4	8
5	3	14	13	7.5	41	20	24
5	4	160	151	76.7	378	100	66
7	2	2	1	0.7	4	6	9
7	3	7	6	3.7	17	42	33
7	4	33	30	18.0	96	294	109
7	5	303	282	182.0	972	2,058	347
11	2	1	1	0.3	2	10	11
11	3	3	3	1.5	9	110	52
11	4	12	12	5.7	30	1,210	215
11	5	59	59	28.2	125	13,310	855
11	6	369	333	216.7	1038	146,410	3,308
13	2	1	1	0.1	2	12	12
13	3	2	2	1.2	6	156	61
13	4	9	9	4.9	22	2,028	276
13	5	37	35	20.7	111	26,364	1,194
13	6	213	208	99.6	469	342,732	5,022
17	2	1	1	0.0	1	16	14
17	3	2	1	0.6	4	272	80
17	4	5	4	3.1	14	4,624	412
17	5	22	20	12.8	70	78,608	2,042
17	6	99	91	50.7	219	1,336,336	9,821
17	7	495	474	249.4	1212	22,717,712	46,277
19	2	1	1	0.0	1	18	15
19	3	1	1	0.6	4	342	89
19	4	4	4	2.2	11	6,498	487
19	5	17	16	8.5	40	123,462	2,550
19	6	82	79	41.1	175	2,345,778	12,969
19	7	336	312	192.7	903	44,569,782	64,607
23	2	1	1	0.0	1	22	17
23	3	1	1	0.3	2	506	108
23	4	3	3	1.9	11	11,638	649
23	5	11	11	6.5	33	267,674	3,737
23	6	50	48	28.0	165	6,156,502	20,909
23	7	211	208	110.5	480	141,599,546	114,604
23	8	1249	1156	553.8	2780	3,256,789,558	618,326

TABLE III
EMPIRICAL TEST OF RANDOM CODES WITH ONE PATCH PER COLUMN.

n	λ	ave	med	stddev	max	$L_{II.1}(n, \lambda)$	$U_{II.6}(n, \lambda, \frac{1}{2})$
5	2	2	2	1.1	6	4	8
5	3	8	8	4.3	19	20	24
5	4	51	48	25.5	119	100	66
7	2	1	1	0.5	3	6	9
7	3	4	4	2.3	11	42	33
7	4	20	17	10.4	64	294	109
7	5	92	86	52.8	248	2,058	347
11	2	1	1	0.1	2	10	11
11	3	2	2	1.2	8	110	52
11	4	8	7	4.1	21	1,210	215
11	5	32	29	16.6	77	13,310	855
11	6	143	131	80.0	497	146,410	3,308
13	2	1	1	0.0	1	12	12
13	3	2	2	0.9	5	156	61
13	4	7	6	3.8	27	2,028	276
13	5	22	19	11.9	62	26,364	1,194
13	6	108	92	55.4	300	342,732	5,022
17	2	1	1	0.0	1	16	14
17	3	1	1	0.6	4	272	80
17	4	4	4	2.4	13	4,624	412
17	5	14	13	6.7	31	78,608	2,041
17	6	57	54	29.2	125	1,336,336	9,821
17	7	229	201	118.3	497	22,717,712	46,277
19	2	1	1	0.0	1	18	15
19	3	1	1	0.4	2	342	89
19	4	3	3	1.7	12	6,498	487
19	5	13	12	6.5	40	123,462	2,550
19	6	51	47	26.7	118	2,345,778	12,969
19	7	210	193	104.9	448	44,569,782	64,607
23	2	1	1	0.0	1	22	17
23	3	1	1	0.3	2	506	108
23	4	3	2	1.5	8	11,638	649
23	5	10	9	4.5	26	267,674	3,737
23	6	35	33	19.4	86	6,156,502	20,909
23	7	138	132	63.3	315	141,599,546	114,604
23	8	568	527	296.3	1422	3,256,789,558	618,326

- 6) Prove a theoretical bound on random codes that applies to general codewords, not just those that randomly select one patch per column as in Theorem II.6.
- 7) Decrease the upper bound on random codes proven in Theorem II.6. The large difference between the medians and the $U_r(n, \lambda, \frac{1}{2})$ numbers in rows of Tables II and III suggest that the $U_r(n, \lambda, \frac{1}{2})$ bound is not tight.
- 8) In defining orthogonality of two macrobonds, we allow them to translate relative to each other and to rotate, but only by 180° . A 2D macrobond based on generalizing the scheme of Figure 1(d) in the most obvious way, in which the blunt ends face orthogonal to the origami face rather than parallel to it as in Figure 1(e), would not have a patch shape that automatically disallows non- 180° rotations.⁴ Thus, it would be interesting to consider adding a rotational constraint to the definition of geometric orthogonal code. For such a macrobond, it would make sense to consider overlaps when a rotation brings points “close” to each other, even if not exactly overlapping. For example, perhaps patch pairs separated by distance at least 1 are far enough apart that they cannot bind (even with distortion as seen in Fig. 1(f)), but those of distance less than 1 (but potentially positive) could bind. Then two macrobonds

⁴As mentioned in Section I-B, there are physical reasons to conjecture that such rotations have weaker stacking bonds than the “standard” rotation.

- have correlation $> \lambda$ if some relative translation and rotation of them brings $> \lambda$ patch pairs to strictly less than distance 1 from each other. In other words, patches behave as diameter-1 circles moving continuously, rather than as width-1 squares moving discretely by integer distances, and correlation corresponds to the number of overlapping circular patches between two macrobonds.
- 9) We model patches as completely non-specific bonds. DNA blunt ends are *relatively* nonspecific, but even so, a GC/CG stack is significantly stronger than an AT/TA stack. The macrobonds employed in [22] use only GC/CG stacks to enforce uniformity, but other stack types are allowed in [13]. One can imagine ways to add some specificity to patches by choice of terminating base pair, or possibly by using DNA sticky ends in place of stacking bonds. The problem is then more accurately modeled by defining a macrobond to be a function $M : [n]^2 \rightarrow C \cup \{\text{null}\}$, where C is a finite set of “colors”, and null represents the absence of a patch. Then, two aligned patches with colors $c_1, c_2 \in C$ have strength $\text{str}(c_1, c_2)$ (for C being the set of possible terminating base pairs, $\text{str}(c_1, c_2)$ is in Table 1 of [18]).
- 10) Our formalization of the concept resembles Figure 1(e) more than 1(d) in the sense that there are two types of faces (“bump” type faces and “dent” type faces), and

a macrobond is always formed between opposite-type faces. In contrast, macrobonds formed in Figure 1(d) are between faces of the same “type.” In this case, one could imagine a macrobond coming into contact with another copy of itself through flipping along one axis only, rather than both axes as captured by our geometric orthogonal flipping codes.

- 11) If we think of the 1D edge of an origami as vertical, then all patches lie at $x = 0$ (since the edge is vertical), and a macrobond chooses a subset of y values at which to place patches. Woo and Rothmund [22] study a related technique for creating specific macrobonds, in which patches are placed at *all possible* y values along the edge, but modifies the *shape* of the edge itself so that some patches lie at different x values; see Fig. 3 of [22]. This sterically prevents all patches from bonding unless the shapes are complementary and aligned properly. So for n patch locations, a code is specified by function $c : [n] \rightarrow \{0, 1, \dots, d\}$, where $d \in \mathbb{N}$ is the maximum allowed “depth” of a patch, relative to the patches that are furthest away from the center of the origami, defined to be at depth 0. It would be interesting to prove upper and lower bounds on code sizes based on n , d , and a desired orthogonality λ (see also [15]).
- 12) Instead of modeling the macrobond as a discrete set of points, model it as a subset $M \subset \mathbb{R}^2$ of the plane. A similar setting was considered by Gopinath, Kirkpatrick, Rothmund, and Thachuk [14], who considered the following problem motivated by experimental problems in nanoscale self-assembly: Design a *shape* S (a bounded, connected subset of \mathbb{R}^2) and a “target” shape T (possibly $T = M$ but not necessarily), such that, starting from any initial placement (translation) of S having with non-zero overlap with T , there is a continuous rigid motion taking S to a unique placement that maximizes the area of overlap between S and T , such that the motion has a monotonically increasing overlap (i.e., there is no local maximum or plateau of suboptimal overlap in which S can get “stuck”). An interesting open problem is to find several (or even *two*) shape-target pairs that have this property, but that also have low cross-correlation. (In this setting auto-correlation is not a concern, since the lack of local maxima or plateaus implies that misaligned translations between a shape and its own target will correct themselves by re-alignment.)

Acknowledgements. We are grateful to Matt Patitz for organizing the 2015 University of Arkansas Self-assembly Workshop, where this project began, and to the participants of that workshop and support from NSF grant CCF-1422152. We thank the participants of the 2015 Workshop on Coding Techniques for Synthetic Biology at the Univ. of Illinois, Urbana-Champaign, especially Han Mao Kiah, Farzad Farnoud, Urbashi Mitra, and Olgica Milenkovic, for bringing optical orthogonal codes to our attention and giving valuable feedback. We thank Paul Rothmund and Sungwook Woo for explaining known physical properties of stacking bonds. We thank anonymous reviewers for comments and pointing out

mistakes in an early draft. We are indebted to Ray Li for correcting several mistakes in the conference version of this paper, in particular for showing how our proof technique for Theorems II.1 and II.2 works only for prime n , not prime powers, and for observing that we require $a_0 = 0$ in each proof as well, changing the bounds in those theorems.

REFERENCES

- [1] Marco Buratti, Koji Momihara, and Anita Pasotti. New results on optimal $(v, 4, 2, 1)$ optical orthogonal codes. *Designs, Codes and Cryptography*, 58(1):89–109, 2011.
- [2] Marco Buratti, Anita Pasotti, and Dianhua Wu. On optimal $(v, 5, 2, 1)$ optical orthogonal codes. *Designs, codes and cryptography*, 68(1-3):349–371, 2013.
- [3] Yanxun Chang, Ryoh Fuji-Hara, and Ying Miao. Combinatorial constructions of optimal optical orthogonal codes with weight 4. *IEEE Transactions on Information theory*, 49(5):1283–1292, 2003.
- [4] Yanxun Chang and Jianxing Yin. Further results on optimal optical orthogonal codes with weight 4. *Discrete mathematics*, 279(1):135–151, 2004.
- [5] Ram Chandra Singh Chauhan, Yatindra Nath Singh, and Rachna Asthana. Design of two dimensional unipolar (optical) orthogonal codes through one dimensional unipolar (optical) orthogonal codes. Technical Report 1309.2254, arXiv, 2013.
- [6] Yuan-Jyue Chen, Benjamin Groves, Richard A. Muscat, and Georg Seelig. DNA nanotechnology from the test tube to the cell. *Nature Nanotechnology*, 10:748–760, 2015.
- [7] Fan Chung, Jawad A. Salehi, and Victor K. Wei. Optical orthogonal codes: Design, analysis and applications. *IEEE Transactions on Information Theory*, 35(3):595–604, May 1989.
- [8] Habong Chung and P Vijay Kumar. Optical orthogonal codes-new bounds and an optimal construction. *IEEE Transactions on Information theory*, 36(4):866–873, 1990.
- [9] Charles J Colbourn and Jeffrey H Dinitz. *Handbook of combinatorial designs*. CRC press, 2006.
- [10] David Doty and Andrew Winslow. Design of geometric molecular bonds. In *ISIT 2016: Proceedings of the IEEE International Symposium on Information Theory*, 2016.
- [11] Ryoh Fuji-Hara and Ying Miao. Optical orthogonal codes: their bounds and new optimal constructions. *IEEE Transactions on Information theory*, 46(7):2396–2406, 2000.
- [12] Gennian Ge and Jianxing Yin. Constructions for optimal $(v, 4, 1)$ optical orthogonal codes. *IEEE Transactions on Information Theory*, 47(7):2998–3004, 2001.
- [13] Thomas Gerling, Klaus F. Wagenbauer, Andrea M. Neuner, and Hendrik Dietz. Dynamic DNA devices and assemblies formed by shape-complementary, nonbase pairing 3D components. *Science*, 347(6229):1446–1452, 2015.
- [14] Ashwin Gopinath, David Kirkpatrick, Paul Rothmund, and Chris Thachuk. Progressive alignment of shapes. In *CCCG 2016: Proceedings of the 28th Canadian Conference on Computational Geometry*, 2016.
- [15] Miriam H. Huntley, Arvind Murugan, and Michael P. Brenner. The information capacity of specific interactions. Technical Report 1602.05649, arXiv, 2016.
- [16] Yu-Chei Lin, Guu-Chang Yang, Cheng-Yuan Chang, and Wing C. Kwong. Construction of optimal 2D optical codes using $(n, w, 2, 2)$ optical orthogonal codes. *IEEE Transactions On Communications*, 59:194–200, 2011.
- [17] Paul W. K. Rothmund. Folding DNA to create nanoscale shapes and patterns. *Nature*, 440(7082):297–302, 2006.
- [18] John SantaLucia Jr and Donald Hicks. The thermodynamics of DNA structural motifs. *Ann. Rev. Biophys. Biomol. Struct.*, 33:415–440, 2004.
- [19] Nadrian C. Seeman. Nucleic-acid junctions and lattices. *Journal of Theoretical Biology*, 99:237–247, 1982.
- [20] E.S. Shivalaleela, A. Selvarajan, and Talabattula Srinivas. Two-dimensional optical orthogonal codes for fiber-optic CDMA networks. *Journal of Lightwave Technology*, 23(2):647–654, Feb 2005.
- [21] Xiaomiao Wang and Yanxun Chang. Further results on optimal $(v, 4, 2, 1)$ -oocs. *Discrete Mathematics*, 312(2):331–340, 2012.
- [22] Sungwook Woo and Paul W. K. Rothmund. Programmable molecular recognition based on the geometry of DNA nanostructures. *Nature Chemistry*, 3:620–627, 2011.
- [23] Jianxing Yin. Some combinatorial constructions for optical orthogonal codes. *Discrete Mathematics*, 185(1):201–219, 1998.